JOURNAL OF COMPUTATIONAL PHYSICS 104, 418-426 (1993)

A Direct Newton Solver for the Two-Dimensional Tokamak Edge Plasma Fluid Equations

D. A. KNOLL, A. K. PRINJA, AND R. B. CAMPBELL*

Chemical and Nuclear Engineering Department, University of New Mexico, Albuquerque, New Mexico 87131

Received January 27, 1991; revised March 5, 1992

Newton's method, finite volume discretization, and a staggered grid are used to compute the steady state profiles of the two-dimensional *two-fluid Tokamak edge plasma fluid equations. In this set of fluid* equations, the transport coefficients are highly nonlinear functions of the dependent variables, and mass and energy transfer due to atomic reactions is included. The techniques of an adaptive damped iteration, mesh sequencing, and reduced factorization are combined to increase the radius of convergence and to accelerate convergence. These techniques are illustrated through a model problem.

1. INTRODUCTION

Advances in supercomputer memory and speed have begun to make Newton's method an attractive choice for two-dimensional computational fluid dynamics (CFD). This has been seen in both the incompressible and compressible flow communities.

In the incompressible flow community Vanka and Leaf [1, 2] have applied Newton's method to two-dimensional laminar and turbulent recirculating flows. In [1] Newton's method was compared to the well-known segregated solution algorithm SIMPLE [3] which uses successive substitution linearization [4]. For driven cavity and sudden expansion model problems, Newton's method was shown to be faster by roughly a factor of five for various Reynolds numbers and grid dimensions, demonstrating the computational speedup to be expected by more accurately modeling the pressure velocity coupling. MacAurther and Patankar [5, 6] have aplied Newton's method and other linearization techniques, with a search parameter to a driven cavity model problem and a natural convection model problem, and compared these to the SIMPLE and SIMPLER [3] algorithms. It was shown that Newton's method with a search parameter could achieve solutions to the natural convection problem for Rayleigh numbers two orders of magnitude greater than those achievable with SIMPLE or SIMPLER, demonstrating the computational robustness to be expected by more accurately modeling the velocity–pressure–temperature coupling of the natural convection problem. In both of these studies constant transport coefficients were used and the Yale sparse matrix package, YSMP [7], was employed to factor and solve the Jacobian.

Venkatakrishnan [8, 9] has applied Newton's method to the compressible two-dimensional Euler and Navier–Stokes equations for airfoil calculations. In this work the ideas of mesh sequencing and reduced factorization have been applied to accelerate convergence and reduce the number of Jacobian factorizations required onthe desired grid refinement. Venkatakrishnan has used both a banded method and YSMP to factor and solve the Jacobian. YSMP has an advantage for the multiply connected grid required for some airfoil computations because it does not require a banded structure.

We would also like to mention the successful application of Newton's method to one-dimensional CFD with complicated physics and chemistry. Winkler, Norman, and Mihalis [10] have applied Newton's method to the equations of adaptive-grid radiation hydrodynamics. Smooke [11] has applied Newton's method to the equations of laminar flames.

In this study we demonstrate the application of Newton's method to another field, namely the two-dimensional, two-fluid equations which model the tokamak edge plasma. This set of equations has transport coefficients which are strong non-linear functions of the dependent variables and incorporates the difficult boundary condition of the plasma sheath with self-consistent neutral particle recycling. Mass and energy transfer due to atomic reactions are also included.

The most widely used edge plasma code is B2 developed by Braams [12], which uses a compressible form of the SIMPLE algorithm. B2 was the pioneering effort in two-dimensional two-fluid edge plasma modeling and has proven to be a useful computational tool for this system of

* Sandia National Laboratories, Division 6428, Albuquerque, NW 87185.

0021-9991/93 $5.00

equations. The desire to more accurately model the physics of the edge plasma has considerably increased the complexity of the edge plasma equations. Attemps to extend B2 to a system of equations with significant concentrations of radiating impurities or a system which includes fluid drifts have met with only limited success [13, 14]. For this reason it is desirable to develop a numerical method for the edge plasma equations which eliminates most of the numerical and physical assumptions of a SIMPLE algorithm, and one such approach is presented here.

We will demonstrate the effects of an adaptive damped iteration, mesh sequencing, and reduced factorization on increasing the radius of convergence and accelerating convergence of Newton's method.

2. EDGE PLASMA FLUID EQUATIONS AND THE MODEL PROBLEM

The tokamak edge plasma (scrape-off layer, boundary layer) is that plasma which lies between the last closed magnetic flux surface, called the separatrix, and the vessel wall. A poloidal cross section of the magnetically diverted double null experiment ASDEX [16] can be seen in Fig. 1. The edge plasma is the shaded region which surrounds the core and impinges on the divertor plates. Energy and particles are transported into the edge region from the core radially across the magnetic separatrix. These flows, once in the edge region, are rapidly transported along the magnetic field lines onto the divertor plates. The energy is deposited on the divertor plates and the plasma ions are neutralized and diffuse back into the plasma as atoms or molecules. These neutrals are ionized by the plasma electrons and charge exchange with plasma ions. The magnetic field is comprised of toroidal and poloidal components, with the toroidal component the stronger of the two. The magnetic field pitch, which is equal to the poloidal field divided by the total field, defines a vector projection from the parallel direction to the poloidal direction. For the model problem [12, 17] the region $\overline{ABCDEF}$ is modeled as a rectangle with the cartesian coordinates x and y representing the poloidal and radial directions, respectively.

The fluid equations of the edge plasma are a simplification of the Braginskii equations [18]. The assumptions are $\mathbf{V}_i = \mathbf{V}_e$, i.e., ambipolar flow, and purely diffusive radial transport. It is also assumed the neutrals which are generated at the divertor plates can be modeled with a single energy diffusion equation [17], and the effects of viscous heating have been ignored. Our problem is then modeled by the following set of steady state equations:

continuity,

$$\frac{\partial n\,u}{\partial x} + \frac{\partial n\,v}{\partial y} = nn_0\langle\sigma\mathbf{v}\rangle_{ie}; \tag{1}$$

neutral diffusion,

$$\frac{\partial}{\partial x}\left(-D_{n_0}\frac{\partial n_0}{\partial x}\right) + \frac{\partial}{\partial y}\left(-D_{n_0}\frac{\partial n_0}{\partial y}\right) = -nn_0\langle\sigma\mathbf{v}\rangle_{ie}; \tag{2}$$

parallel momentum,

$$\frac{\partial}{\partial x}\left(mnuu_{\|} - \eta_x\frac{\partial u_{\|}}{\partial x}\right) + \frac{\partial}{\partial y}\left(mnvu_{\|} - \eta_y\frac{\partial u}{\partial y}\right) = -\frac{B_x}{B}\left(\frac{\partial P_i}{\partial x} + \frac{\partial P_e}{\partial x}\right); \tag{3}$$

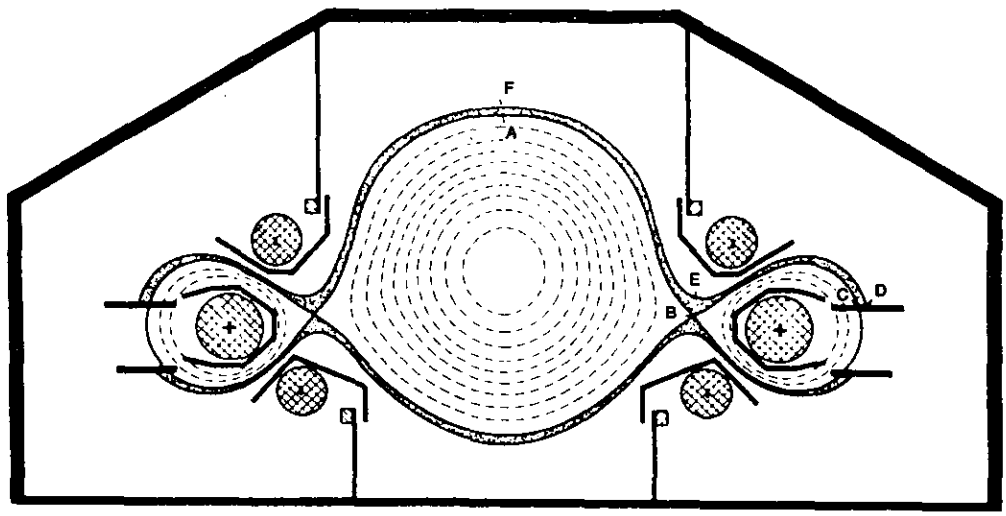

FIG. 1. ASDEX tokamak poloidal cross section.

ion internal energy,

$$\frac{\partial}{\partial x}\left(\frac{3}{2}nuT_i-\kappa_x^i\frac{\partial T_i}{\partial x}\right)+\frac{\partial}{\partial y}\left(\frac{3}{2}nvT_i-\kappa_y^i\frac{\partial T_i}{\partial y}\right)$$
$$=-P_i\left(\frac{\partial u}{\partial x}+\frac{\partial v}{\partial y}\right)+\kappa_{eq}(T_e-T_i)+\varepsilon_i nn_0\langle\sigma\mathbf{v}\rangle_{ie}; \quad (4)$$

electron internal energy,

$$\frac{\partial}{\partial x}\left(\frac{3}{2}nuT_e-\kappa_{\lim}^e\frac{\partial T_e}{\partial x}\right)+\frac{\partial}{\partial y}\left(\frac{3}{2}nvT_e-\kappa_y^e\frac{\partial T_e}{\partial y}\right)$$
$$=-P_e\left(\frac{\partial u}{\partial x}+\frac{\partial v}{\partial y}\right)-\kappa_{eq}(T_e-T_i)-\varepsilon_e nn_0\langle\sigma\mathbf{v}\rangle_{ie}; \quad (5)$$

equation of state,

$$P_i=nT_i, \qquad P_e=nT_e. \quad (6)$$

Here n is the plasma density, n_0 is the neutral density, $u_{||}$ is the velocity along the total magnetic field, B. T_i is the ion temperature, T_e is the electron temperature, and B_x/B is the magnetic field pitch. To close this set of equations we have

radial velocity,

$$v=-\frac{D_{ni}}{n}\frac{\partial n}{\partial y}; \quad (7)$$

poloidal velocity,

$$u=\frac{B_x}{B}u_{||}. \quad (8)$$

Note that in Eqs. (7) and (8) we have ignored the effects of fluid drifts [19, 20]. In this model the poloidal transport coefficients are classical Braginskii [18] and the radial transport coefficients are anomalous, i.e., empirical. The poloidal electron thermal conductivity is flux limited by the electron thermal velocity to keep the electron diffusive heat flux in a physically reasonable range [12, 17]. In a nearly collisionless plasma with steep temperature gradients, the continuum formulation of the diffusive energy flux can be unrealistic. Since diffusion is a random walk process, the diffusive energy flux cannot exceed the energy flux that can be convected at the local thermal speed of the particles. We have

$$\kappa_{\lim}^e=\frac{\kappa_x^e}{1+q_x/q_{fl}} \quad (9)$$

with

$$q_x=-\kappa_x^e\frac{\partial T_e}{\partial x} \quad (10)$$

and

$$q_{fl}=0.2nT_e\sqrt{T_e/m_e}. \quad (11)$$

The neutral diffusion coefficient is developed from diffusion theory assuming thermal equilibrium between neutrals and plasma ions [17]. The functional dependencies of the transport coefficients are:

X-direction (poloidal) transport,

$$\kappa_x^e\propto\frac{T_e^{2.5}}{m_e}, \qquad \kappa_x^i\propto\frac{T_i^{2.5}}{m_i}, \qquad \eta_x\propto T_i^{2.5};$$

Y-direction (radial) transport,

$$\kappa_y^e\propto\chi_e n, \quad \kappa_y^i\propto\chi_i n, \quad \eta_y\propto\eta_\perp nm_i$$

with D_{ni}, χ_i, χ_e, $\eta_\perp$, input empirical constants. The thermal equipartition coefficient is given by

$$\kappa_{eq}\propto\frac{m_e n^2}{m_i T_e^{1.5}} \quad (12)$$

and the neutral diffusion coefficient is defined as

$$D_{n_0}=\frac{T_i}{3nm(\langle\sigma\mathbf{v}\rangle_{ie}+\langle\sigma\mathbf{v}\rangle_{cx})}. \quad (13)$$

The source and sink terms due to neutral ionization depend on the electron impact ionization rate, $\langle\sigma\mathbf{v}\rangle_{ie}$, which is a function of electron temperature,

$$\langle\sigma\mathbf{v}\rangle_{ie}=\frac{3\times10^{-14}a^2}{3+a^2}\frac{\mathrm{m}^3}{\mathrm{s}}, \quad a=\frac{T_e\,\mathrm{eV}}{10}. \quad (14)$$

The constants ε_i and ε_e represent the energy lost or gained due to the electron impact of hydrogen atoms. We also assume that the charge exchange rate, $\langle\sigma\mathbf{v}\rangle_{cx}$, is a constant for this model problem. Equations (1) through (5), along with the given transport coefficients, represent a strongly coupled nonlinear system of fluid equations. As we see below in the model problem, the boundary conditions at the divertor plate, where the neutrals are produced, only serve to increase the coupling and nonlinearity of the problem. The geometry of the model problem is the region $\overline{ABCDEF}$ of Fig. 1 modeled as a rectangle with x being the poloidal coordinate and y being the radial coordinate. This can be seen in Fig. 2. We use the following boundary conditions:

symmetry plane ($\overline{AF}$),

$$u_{||}=0, \quad \frac{\partial n}{\partial x}=\frac{\partial n_0}{\partial x}=\frac{\partial T_i}{\partial x}=\frac{\partial T_e}{\partial x}=0;$$

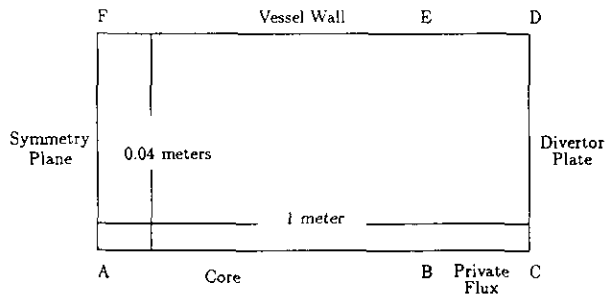

FIG. 2. Model problem geometry.

vessel wall ($\overline{FD}$),

$$\frac{\partial u_{\|}}{\partial y}=\frac{\partial n}{\partial y}=\frac{\partial n_0}{\partial y}=\frac{\partial T_i}{\partial y}=\frac{\partial T_e}{\partial y}=0$$

between E and D (γ = albedo = 0.9),

$$-D_{n_0}\frac{\partial n_0}{\partial y}=0.5\,\frac{1-\gamma}{1+\gamma}\,n_0\sqrt{\frac{T_i}{m_i}};$$

core ($\overline{AB}$),

$$u_{\|}=0,\quad n=1.8\times 10^{19}\ \mathrm{m}^{-3},\quad \frac{\partial n_0}{\partial y}=0,\quad T_i=T_e=80\ \mathrm{eV};$$

private flux ($\overline{BC}$, $\Gamma_{i,e}$ = energy scale length),

$$\frac{\partial u_{\|}}{\partial y}=\frac{\partial n}{\partial y}=\frac{\partial n_0}{\partial y}=0,\quad \frac{\partial T_i}{\partial y}=\Gamma_i,\quad \frac{\partial T_e}{\partial y}=\Gamma_e$$

with

$$\Gamma_i=(-75\ \mathrm{m/s})\,nT_i,\quad \Gamma_e=(-150\ \mathrm{m/s})\,nT_e.$$

divertor plate ($\overline{DC}$) (sheath boundary),

$$u_{\|}=C_s=\sqrt{(T_i+T_e)/m_i},\qquad D_{n_0}\frac{\partial n_0}{\partial x}=\frac{B_x}{B}\,nC_s,$$

$$\mathbf{q}_i=2.5\,\frac{B_x}{B}\,nC_sT_i,\quad \mathbf{q}_e=4.5\,\frac{B_x}{B}\,nC_sT_e,$$

where

$$\mathbf{q}_{i,e}=1.5nuT_{i,e}-\kappa_{i,e}(\partial T_{i,e}/\partial x).$$

The input constants are

$$D_{ni}=2,\quad \chi_i=0.2,\quad \chi_e=4.0,\quad \eta_\perp=0.2,\ \mathrm{m}^2/\mathrm{s};\ B_x/B=0.06.$$

The boundary along the separatrix from the null point to the divertor plate is called the private flux boundary. Along the private flux boundary a net loss of energy is assumed with no net loss of particles. Along the vessel wall between point E and D there is a net outflux of neutrals governed by an albedo boundary condition. The boundary condition at the plate is the most complicated and is arrived at from plasma sheath theory [21]. Here the neutral flux is assumed to be equal in magnitude and opposite in direction to the plasma flux, corresponding to all plasma ions neutralizing at the plate and forming a source of neutrals.

3. NEWTON'S METHOD

The solution of Eqs. (1) through (5) with appropriate boundary conditions is a difficult task. However, to properly model the tokamak edge plasma we also need to solve an equation for the electrostatic potential and include $\mathbf{E}\times\mathbf{B}$ and diamagnetic fluid drifts in Eqs. (7) and (8). It will also be necessary to include impurity fluids, such as carbon eroded from the divertor plates, in the model. For this reason, it is desirable to develop a very robust nonlinear solver for this system. By using Newton's method and solving all equations simultaneously, the least number of physical and numerical assumptions possible are made. The main challenge in using Newton's method for two-dimensional CFD, assuming the required memory is available, is increasing the radius of convergence and accelerating convergence so that the large Jacobian is factored as few times as possible. Of course, for many problems it may also be a challenge to keep the condition number of the Jacobian in a reasonable range.

We use finite volume discretization on Eqs. (1) through (5) on a staggered grid with velocities at cell faces and thermodynamic variables at cell centers. This produces a nonlinear matrix equation:

$$\mathbf{A}(\mathbf{x})=\mathbf{b}, \tag{15}$$

where $\mathbf{x}$ is our state vector and $\mathbf{A}$ is a function of the state vector. In Newton's method, Eq. (15) is approximated by a first-order Taylor series giving

$$\mathbf{J}\,\delta\mathbf{x}=\mathbf{res}, \tag{16}$$

where the (i, j) element of the Jacobian matrix, $\mathbf{J}$, is given by

$$J(i,j)=-\frac{\partial res(i)}{\partial x(j)} \tag{17}$$

and

$$\mathbf{res}=\mathbf{b}-\mathbf{A}(\mathbf{x}) \tag{18}$$

is the residual. Equation (16) is then solved in the following iterative fashion:

$$\mathbf{J}^k \delta \mathbf{x}^k = \mathbf{res}^k \tag{19}$$

$$\mathbf{x}^{k+1} = \mathbf{x}^k + \delta \mathbf{x}^k. \tag{20}$$

This is done until the norm of $\mathbf{res}^k$ falls below some tolerance level with **J** and **res** being recomputed each time **x** is updated.

Currently we employ banded Gaussian elimination to solve the linearized problem. The LINPACK [24] routines SGBFA and SGBSL are used. The storage required can be computed using the grid dimensions, *nx* and *ny*, and the number of conservation equations being solved, *neq*. The total number of finite volume equations being solved is $nx * ny * neq$. We form the Jacobian with *j*, the *y* direction, being the fastest changing index to minimize the bandwidth since, for our application, *nx* is always greater than *ny*. The half bandwith, *hbw*, of our Jacobian is given by $(ny+1) * neq$. The LINPACK routines require $(3 * hbw + 3) * nx * ny * neq$ words of memory for the matrix, the pivot vector, and the right-hand side.

It is known that the radius of convergence of Newton's method is inversely proportional to the dimension of Eq. (16) [22]. It is also known that an accurate initial guess, $\mathbf{x}^0$, to the true solution, **x**, will greatly accelerate convergence of Newton's method. Mesh sequencing is used to take advantage of these two facts. We begin our computation on a grid which is coarser than the desired final resolution, but which is fine enough to capture the basic physical structure of the solution. Starting from an initial guess on the coarse grid, we expect to have an increased radius of convergence, compared to starting with the same initial guess on a much finer grid since the dimension of Eq. (16) is reduced. After converging to a solution on this grid, the grid dimension is doubled and the converged solution is interpolated up to the new grid, providing a much improved initial guess for the new grid. This procedure is continued until a grid of the desired refinement is reached, in a manner somewhat analogous to the first upward cycle of a full multigrid scheme [15], except that we solve the problem on each grid of increasing resolution.

Because there is a limit on the coarseness of the initial grid, we may still have a problem with a small radius of convergence. To increase the radius of convergence further for an initial guess, a damped iteration is employed. By a damped iteration we mean Eq. (20) is altered to

$$\mathbf{x}^{k+1} = \mathbf{x}^k + s\,\delta \mathbf{x}^k, \tag{21}$$

where *s* is a scalar less than or equal to one. There are a variety of ways in which *s* can be defined. One way is to define *s* so as to minimize the Euclidean norm of **res** [22], which is closely related to the search parameter used by MacArthur and Patankar [5, 6]. This procedure will increase in complexity as the complexity of **res** increases. Since our residual vector is more complicated than those of the model problems studied by MacArthur and Patankar, we have opted for a simpler procedure similar to that used by Winkler *et al.* [10]. In this procedure *s* is defined by

$$s = \min\left[1, \min_{i,j,k}\left(\frac{\alpha * x_{i,j,k}}{\delta x_{i,j,k}}\right)\right], \tag{22}$$

where the indices (i, j) run over all control volumes and the index *k* runs over all dependant variables, except velocity. With this search parameter no thermodynamic variable is allowed to change by more than a fixed fraction, α, in any Newton iteration. This method also serves to prevent any thermodynamic variable from becoming negative. As the solution is approached and δx becomes small, *s* will become one and a full Newton update will be taken.

We also employ the idea of a modified Newton iteration [4], referred to as reduced factorization. In Eq. (19) the Jacobian is not evaluated and factored at every iteration, but instead the LU factorization of a Jacobian may be used two or more times in succession. This can save a tremendous amount of CPU time since factoring **J** can represent as much as 95% of a Newton iteration. Smooke [11] has developed a computable test which determines when a new Jacobian needs to be computed and factored to ensure that $\mathbf{res} \to 0$. Currently, we fix the frequency of computing a new Jacobian and we compute a new Jacobian at every iteration when the search parameter, *s*, is not equal to one.

For the above "standard" edge plasma model we use an analytically defined Jacobian. Although this is a cumbersome task to code and debug, especially because of the boundary conditions, once successfully completed it saves significant CPU time over numerically evaluating the Jacobian. Currently, our analytic Jacobian does not include derivatives of the flux-limited electron conductivity. As we move to a more complicated system of equations including fluid drifts and impurities we well evaluate the Jacobian numerically [23].

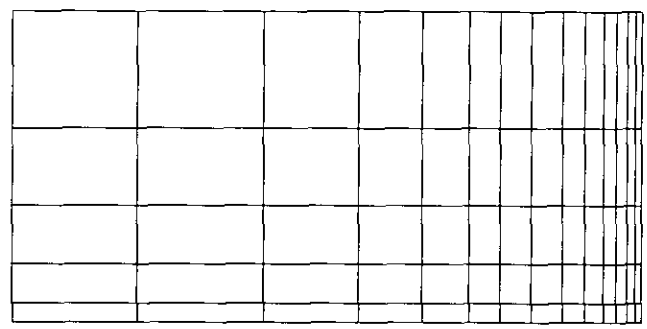

FIG. 3. Structure of nonuniform grid.

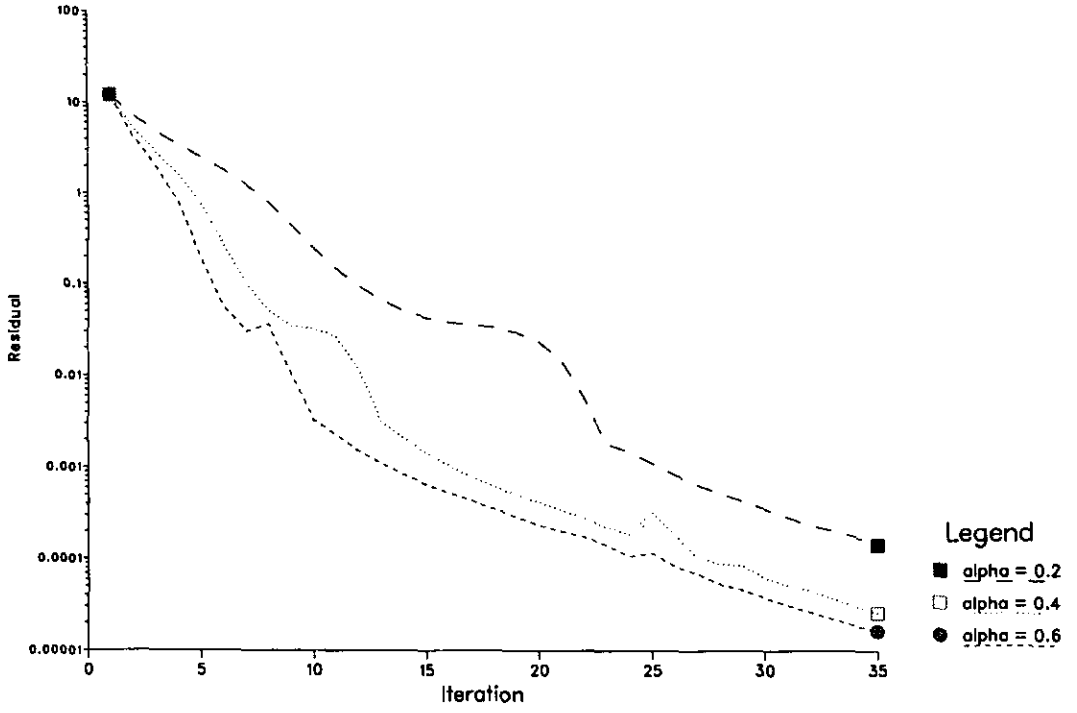

FIG. 4. Effect of damping on convergence.

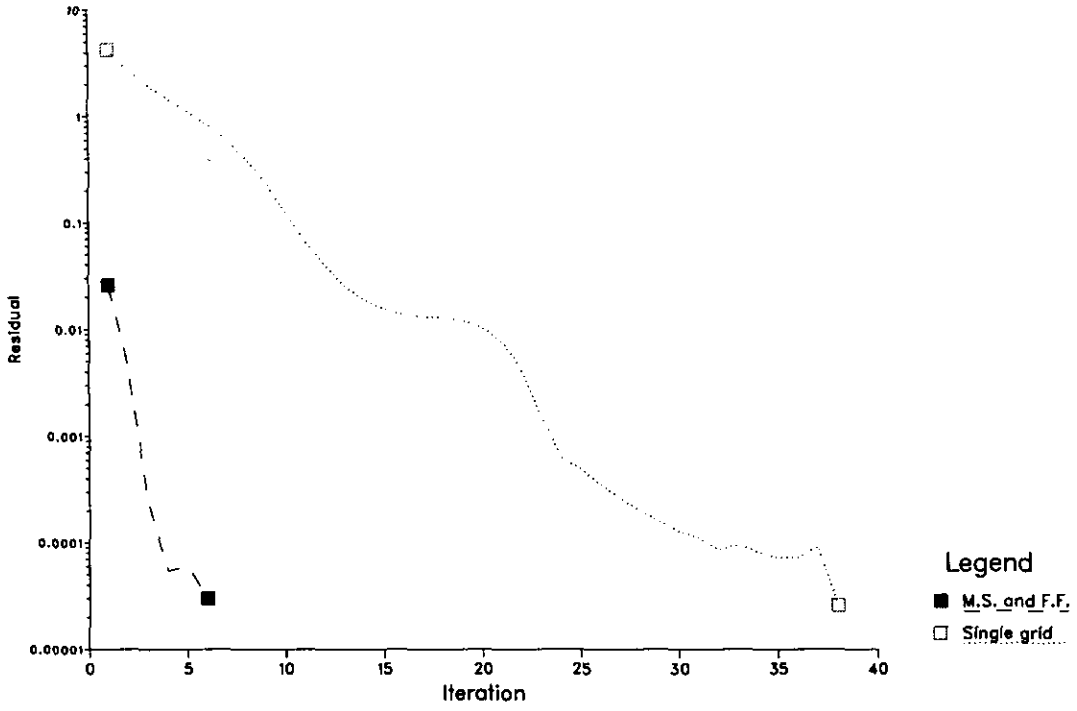

FIG. 5. Effect of mesh sequencing and reduced factorization.

4. RESULTS FROM MODEL PROBLEM

The model problem as been chosen because it has been part of two previous studies of edge plasma codes [12, 17]. We are most interested in demonstrating convergence characteristics. The solution on the rectangle of Fig. 2 is characterized by sharp radial gradients near the separatrix and sharp poloidal gradients near the divertor plate. For this reason we use a nonuniform grid shown in Fig. 3. This is a 14×5 grid which is the initial grid for our mesh sequencing. To construct a 28×10 grid each control volume is divided in half in both the x and y directions.

We first want to illustrate the performance that can be expected in this type of problem. We follow a root mean squared normalized residual for the system of finite volume equations including the boundaries. The normalization is such that when the residual for the dependent variable ϕ is less than 1.0×10^{-4}, we have $\delta\phi/\phi$ less than 1.0×10^{-8} which we consider converged. Figure 4 shows the convergence history for a flat initial profile on a 28×10 grid for various α's in Eq. (22). We can see that $\alpha = 0.4$ is an improvement over $\alpha = 0.2$, but beyond that there is not much difference. Also, we should point out that, if no damping is used, divergence occurs. As we move to more complicated physics such as radiating impurities [23] we expect that a more restrictive value of α may be required for convergence. It should also be noted that we do not achieve quadratic convergence. This is because we have omitted some of the more complicated derivatives from our analytical Jacobian, and thus we have an approximate Jacobian. Work on implementing an efficient numerically evaluated Jacobian is currently underway.

Next, we want to illustrate the effect of mesh sequencing and reduced factorization. A 56×20 grid and $\alpha = 0.4$ will be used for this. The Jacobian will be factored every iteration when s in Eq. (22) is not equal to one, every other iteration when $s = 1$, and factorization will be completely frozen when the residual is less than 5.0×10^{-5}. Figure 5 compares the convergence history on the 56×20 grid for a single grid computation and no reduced factorization to a mesh sequencing computation using reduced factorization. In the mesh sequencing computation the problem was first solved on a 14×5 grid and then a 28×10 grid to give the much improved initial guess to the 56×20 grid problem seen in Fig. 5. The convergence history for the mesh sequencing problem required six fine-grid iterations for convergence; however, the Jacobian was only factored on three of these iterations. The total CPU time required on the 14×5 and 28×10 grids was equivalent to the cost of one fine-grid iteration. Thus a converged solution on the 56×20 grid, using mesh sequencing and reduced factorization, required four fine-grid iterations, compared to the 38 iterations required for the single grid computation. The actual Cray 2 CPU time for these two runs using standard LINPACK

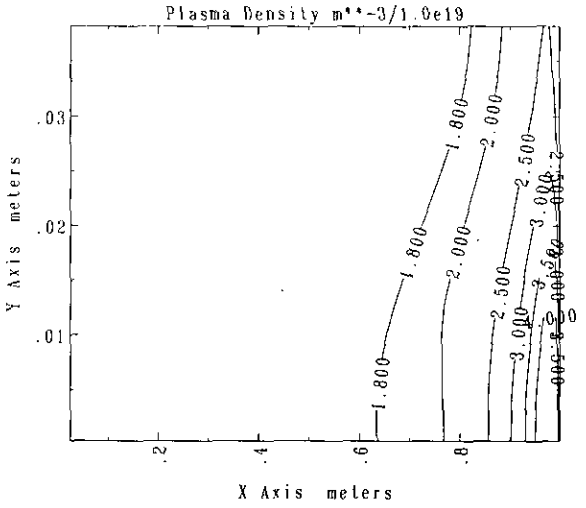

FIG. 6. Density on 56×20 grid.

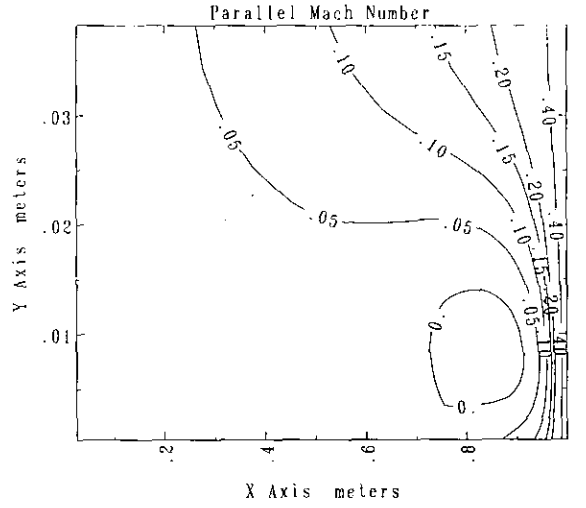

FIG. 7. Parallel Mach number on 56×20 grid.

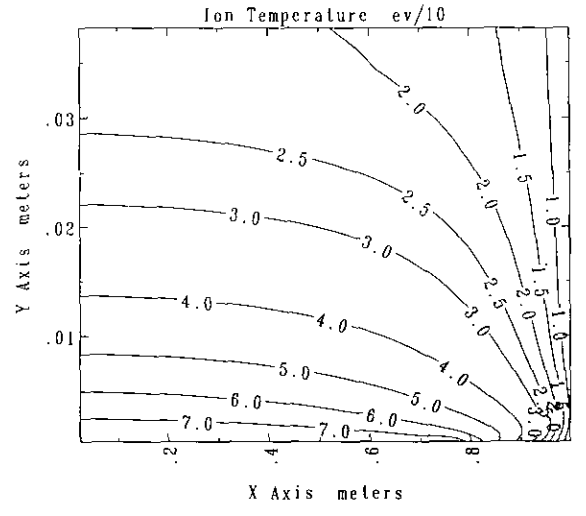

FIG. 8. Ion temperature on 56×20 grid.

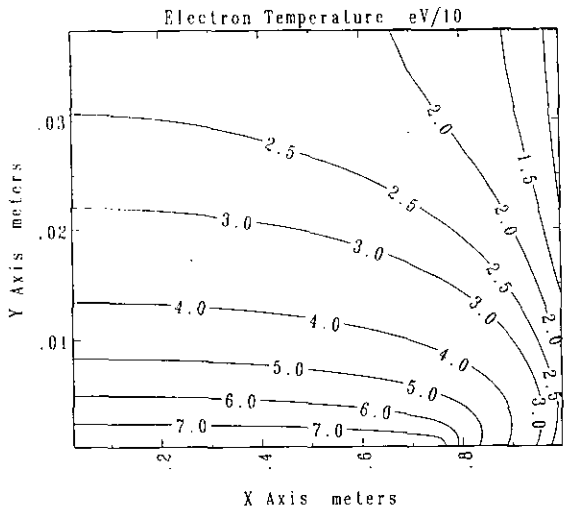

FIG. 9. Electron temperature on 56×20 grid.

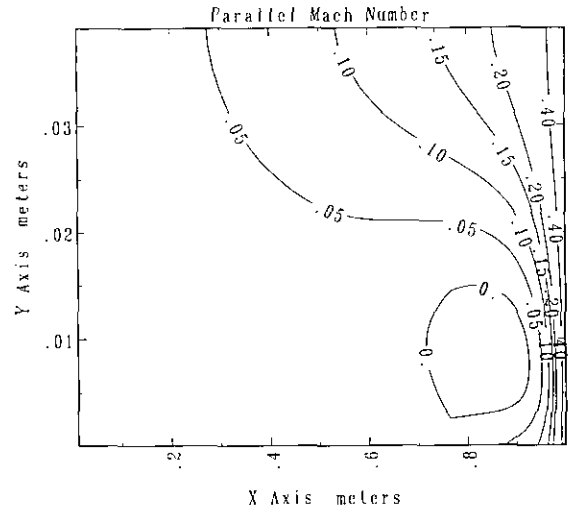

FIG. 11. Parallel Mach number on 112×40 grid.

banded solvers was 26 and 250 s. Thus mesh sequencing and reduced factorization represent an order of magnitude in computational speedup for this model problem.

The solution profile of this model problem will now be examined. Figures 6 through 9 are contour plots of density, parallel Mach number, ion and electron temperature on a 56×20 grid using upwind differencing for convection. The plots show the typical results [12, 17] of density buildup near the divertor plate, sharp radial temperature gradients near the separatrix, sharp poloidal gradients in temperature, density, and Mach number near the divertor plate, and a sone of flow reversal near the divertor plate caused by the neutral recycling. We will now double the grid dimension in both directions to 112×40. Figures 10 and 11 are the contour plots of density and parallel Mach number. These plots show very little difference from the 56×20 results. Both these sets of results agree well with the results

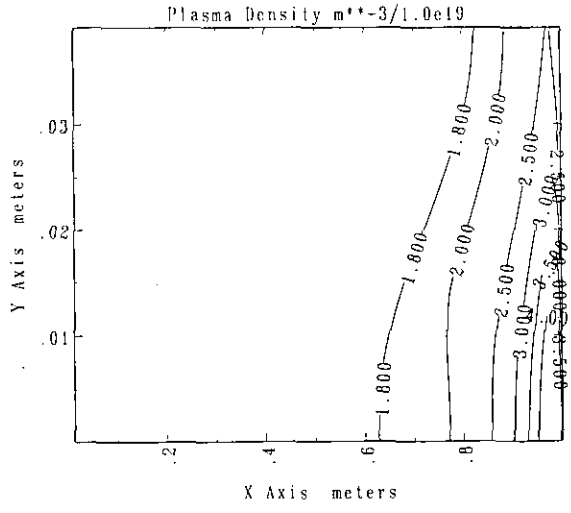

FIG. 10. Density on 112×40 grid.

of Vold [17], who also solves a neutral diffusion equation. Vold computed a peak density near the plate of $4.5 \times 10^{19}\ m^{-3}$, where we have a peak density near the plate of $5.0 = 10^{19}\ m^{-3}$. The same computation of Braams [12] assumed a fixed ion and electron temperature of 2 eV at the wall and used a different neutral model. In this computation the peak density near the plate was $5.5 \times 10^{19}\ m^{-3}$. It should be pointed out that both Braams and Vold used the power law differencing scheme of Patankar [3] for the convection diffusion operators while we have used upwind differencing for convection and central differencing for diffusion.

5. CONCLUSIONS

We have demonstrated that Newton's method coupled with a damped iteration, mesh sequencing, and reduced factorization is a CPU-efficient solution procedure for the nonlinear coupled system of fluid equations of the Tokamak edge plasma. It is a very robust scheme since it makes the fewest possible numerical and physical assumptions, but it is limited by memory requirements. To store and factor the Jacobian for the 112×40 grid using LINPACK-banded solvers requires approximately 15 megawords decimal on the Cray 2. In the future we will examine reducing this requirement by moving to a more memory-efficient large sparse-matrix package such as YSMP or MA32 [25].

Future development of this tool will involve curvilinear orthogonal coordinates, automation of the reduced factorization, implementation of an efficient numerically evaluated Jacobian, and the inclusion of advanced physics such as fluid drifts and radiating impurities.

REFERENCES

1. S. P. Vanka and G. K. Leaf, ANL-83-73, Argonne National Laboratory, 1983.

2. S. P. Vanka, *Int. J. Heat Mass Transfer* **28**, 2093 (1985).
3. S. V. Patankar, *Numerical Heat Transfer and Fluid Flow* (Hemisphere, New York, 1980).
4. J. S. Vandergraft, *Introduction to Numerical Computations* (Academic Press, New York, 1983).
5. J. W. MacArthur and S. V. Patankar, *Int. J. Num. Meth. Fluids* **9**, 325 (1989).
6. J. W. MacArthur, Ph.D. thesis, University of Minnesota, 1986.
7. S. G. Eisenstat *et al.*, Technical Report 114, Department of Computer Science, Yale University, 1978.
8. V. Venkarakrishnan, *AIAA J.* **27**, 885 (1989).
9. V. Venkatakrishnan, *Comput. Fluids* **18**, 191 (1990).
10. K. A. Winkler, M. L. Norman, and D. Mihalas, in *Multiple Time Scales*, edited by J. U. Brackbill and B. I. Cohen (Academic Press, New York, 1985).
11. M. D. Smooke, *J. Comput. Phys.* **48**, 72 (1982).
12. B. J. Braams, Ph.D. Thesis, University of Utrecht, 1986.
13. D. A. Knoll, A. K. Prinja, and B. J. Braams, *Bull. Am. Phys. Soc.* **35** (1989).
14. B. J. Braams and D. P. Coster, *Bull. Am. Phys. Soc.* **35** (1990).
15. A. Brandt, technical report, von Karman Institute, 1984 (unpublished).
16. J. Wesson, *Tokamaks* (Clarendon Press, Oxford, 1987).
17. E. L. Vold, Ph.D. thesis, University of California, Los Angeles, 1989.
18. S. I. Braginskii, *Reviews of Plasma Physics* (Consultants Bureau, New York, 1985).
19. D. A. Knoll and A. K. Prinja, *J. Nucl. Mat.* **176 & 177**, 562 (1990).
20. M. Petravic and G. Kuo-Petravic, *Nucl. Fusion* **30**, 1148 (1990).
21. P. C. Stangeby, in *Physics of Plasma Wall Interactions in Controlled Fusion*, edited by Post and Behrisch (Plenum, New York, 1984).
22. C. A. J. Fletcher, *Computational Techniques for Fluid Dynamics, Vol. I* (Springer-Verlag, Berlin, 1988).
23. R. B. Campbell, D. A. Knoll, and A. K. Prinja, *Bull. Am. Phys. Soc.* **35** (1990).
24. J. Dongarra, J. Bunch, C. Moler, and G. Stewart, *LINPACK User's Guide*, (SIAM, Philadelphia, 1979).
25. I. S. Duff, Technical Report AERE-R 10079, AERE Harwell, 1981.